Ji Wang
State Key Laboratory of Mechanical Transmission, and College of Automotive, Engineering, Chongqing University, Chongqing 400044, China
e-mail: wangji@cqu.edu.cn

Shumon Koga
Department of Mechanical and Aerospace Engineering, University of California, San Diego, La Jolla, CA 92093-0411
e-mail: skoga@ucsd.edu

Yangjun Pi
State Key Laboratory of Mechanical Transmission, and College of Automotive, Engineering, Chongqing University, Chongqing 400044, China
e-mail: cqpp@cqu.edu.cn

Miroslav Krstic
Fellow ASME
Department of Mechanical and Aerospace Engineering, University of California, San Diego, La Jolla, CA 92093-0411
e-mail: krstic@ucsd.edu

Axial Vibration Suppression in a Partial Differential Equation Model of Ascending Mining Cable Elevator

Lifting up a cage with miners via a mining cable causes axial vibrations of the cable. These vibration dynamics can be described by a coupled wave partial differential equation-ordinary differential equation (PDE-ODE) system with a Neumann interconnection on a time-varying spatial domain. Such a system is actuated not at the moving cage boundary, but at a separate fixed boundary where a hydraulic actuator acts on a floating sheave. In this paper, an observer-based output-feedback control law for the suppression of the axial vibration in the varying-length mining cable is designed by the backstepping method. The control law is obtained through the estimated distributed vibration displacements constructed via available boundary measurements. The exponential stability of the closed-loop system with the output-feedback control law is shown by Lyapunov analysis. The performance of the proposed controller is investigated via numerical simulation, which illustrates the effective vibration suppression with the fast convergence of the observer error. [DOI: 10.1115/1.4040217]

Keywords: wave equation, PDE-ODE, moving boundaries, backstepping, vibration control

1 Introduction

1.1 Control of Mining Elevators. Compliant varying-length cable systems are widely applied in numerous industries, such as elevators and hoisters [1,2]. The cable's property of "compliance" or its ability to "stretch" and contract causes mechanical vibrations especially in the ascending process when the vibratory energy is increasing [3,4], which leads to imprecise positioning and premature fatigue fracture. For the safe manipulation, vibration suppression is important to avoid serious hazards. Hence, an effective and feasible control design for vibration suppression of the varying-length compliant cable system lifting a cage shown in Fig. 1 is required, where the vibration dynamics of the cable elevator is modeled as a distributed parameter system [2–5].

1.2 Control of Vibrating String/Cable Systems With Fixed and Moving Boundaries. The vibrating string is an infinite dimensional system described by a wave partial differential equation (PDE). Most of the existing studies about vibration control of compliant strings focus on the fixed length. An active boundary control scheme was proposed in Refs. [6–8] to suppress the vibrations and regulate the transport velocity of the axially moving string system. In Refs. [9] and [10], the boundary control based on an integral barrier Lyapunov function was used to suppress the undesirable vibrations of the compliant string system. To guarantee stability under the uncertainty of the model, a robust adaptive boundary control was developed in Ref. [11] for a class of compliant string systems under the unknown spatiotemporally varying distributed disturbance and the time-dependent boundary disturbance. In Ref. [12], an adaptive boundary controller was designed to suppress vibrations and control tension of a flexible marine riser. A cooperative control law based on the novel integral-barrier Lyapunov function was proposed for a nonuniform fixed-length gantry crane where the uncertain parameters were handled by two adaption laws in Ref. [13]. An "impedance matching" method [14], where the transfer functions of distributed parameter systems can be obtained through Laplace transforms and the pole and zero locations are to be matched by the control input design, was successfully applied in a fixed domain wave PDE, which is a linear time-invariant system describing a vibrating string with a constant length L.

The time-varying length has a significant role on the vibration dynamic characteristics of compliant string systems [3,15] and makes the design of the controller more challenging. There are relatively few studies dealing with vibration control problems of varying-length cables. The control problems for horizontally and vertically translating media with the varying length were investigated in Ref. [16]. A boundary control scheme was designed to suppress the vibrations for a nonlinear varying length drilling riser system in Ref. [17]. In Ref. [18], a boundary control law was developed to stabilize the transverse vibrations of a nonlinear vertically moving string system with the varying length. However, in the literature, the actuators are required to follow the moving cage, which is difficult to achieve in the practical implementation due to the inconvenient installation.

From a practical point of view, a control system where control is applied through the fixed boundary opposite to the instability is needed in the mining cable elevator. This is a more challenging task than the classical collocated "boundary damper" feedback control [19]. In Ref. [19], a control problem for the stabilization of an one-dimensional hyperbolic equation, which contains the instability at its free end and the control input on the opposite end, was dealt with by using the backstepping method [20]. In Ref. [21], the first global result was proposed for hyperbolic equations where the actuator is not collocated with the source of the instability. In Refs. [22] and [23], adaptive control laws were developed

Contributed by the Dynamic Systems Division of ASME for publication in the Journal of Dynamic Systems, Measurement, and Control. Manuscript received October 10, 2017; final manuscript received May 2, 2018; published online June 4, 2018. Assoc. Editor: Davide Spinello.

Copyright © 2018 by ASME

Downloaded From: http://dynamicsystems.asmedigitalcollection.asme.org/ on 06/16/2018 Terms of Use: http://www.asme.org/about-asme/terms-of-use

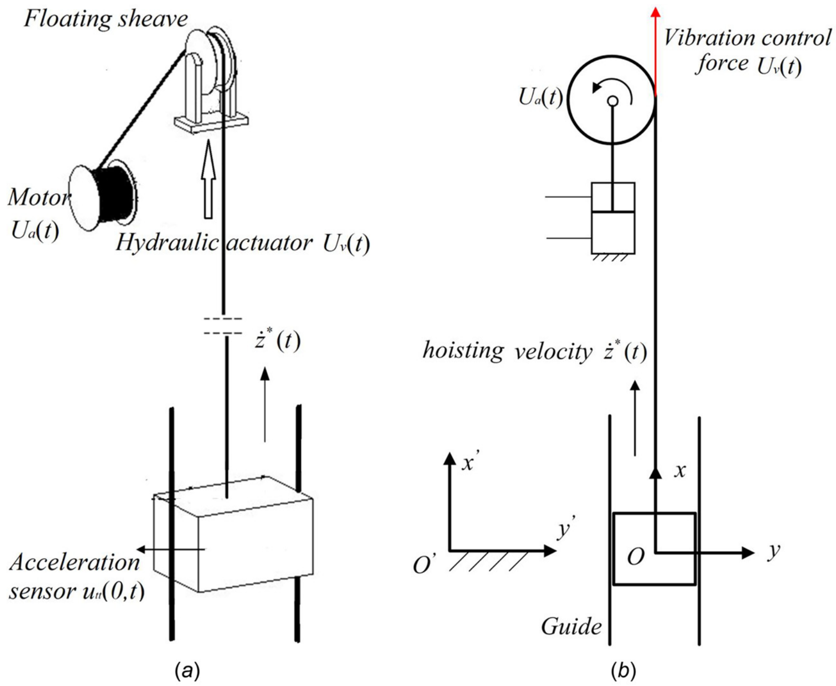

Fig. 1 The mining cable elevator: (*a*) original model and (*b*) simplified model

for one-dimensional hyperbolic equations, which had an actuator on one boundary and the unknown anti-damping on the other boundary. However, the spatial domain of their system is limited to be constant in time.

1.3 Control of Partial Differential Equation-Ordinary Differential Equation Systems. The mathematical model of vibration control for a varying-length string with a moving cage can be formulated as stabilizing a coupled wave partial differential equation-ordinary differential equation (PDE-ODE) system on a time-varying spatial domain with an uncontrolled Neumann type interface, as shown in this paper. For control design of PDE-ODE cascades, compensation of actuator dynamics governed by a heat PDE and a wave PDE was developed by Krstic [24] and [25], respectively. Designs of the boundary observer and the output feedback controller for a class of hyperbolic PDE-ODE cascade systems were developed in Refs. [26] and [27]. As a more challenging problem, coupled PDE-ODE systems where the PDE state and the ODE state act back simultaneously have been studied. In Ref. [28] and [29], the coupled heat PDE-ODE systems with Dirichlet type uncontrolled interconnections were stabilized via the backstepping transformations. By the decomposition of the wave equation into two transport equations, the stabilization of a nonlinear ODE with actuator dynamics governed by a wave PDE through the Dirichlet interconnection on the moving boundary was developed in Refs. [30] and [31] based on the predictor-based feedback control. However, the compensation of actuator dynamics of a wave PDE through the Neumann type interconnection is more challenging. In Ref. [32], a PDE-ODE cascade system was extended from the Dirichlet type interconnection to the Neumann type interconnection. The control designs of coupled heat-ODE and wave-ODE systems including the Neumann type interconnections were further developed in Refs. [33] and [34], respectively, which focused on the fixed domain PDE with the Dirichlet type actuation.

1.4 Results of the Paper

(1) Axial vibration dynamics of a mining cable elevator is modeled as a PDE system by Hamilton's principle in Sec. 2.
(2) A state-feedback controller with explicit gain kernels is designed to stabilize the coupled wave PDE-ODE system on a time-varying spatial domain with a Neumann type interconnection, which is shown in Sec. 3.
(3) A finite-dimensional observer with explicit gain kernels is also designed to estimate the full distributed states of the varying-length string only using measurable boundary states in an anti-collocated setup, which is shown in Sec. 4.
(4) The exponential stability of the observer-based output-feedback control system is proved via Lyapunov analysis in Sec. 5. The result is verified via numerical simulations in Sec. 6 before the conclusions and future work in Sec. 7.

1.5 Contributions of the Paper

(1) We extend the result in Sec. 6 of Ref. [32], which stabilized a cascaded wave PDE-ODE system on a fixed domain via a full-state feedback controller to the stabilization of a coupled wave PDE-ODE system on a time-varying spatial domain via an observer-based output-feedback controller.
(2) Compared with previous contributions for the wave PDE-ODE system with a Dirichlet type interconnection on a free boundary studied in Refs. [30] and [31] which exploited the stabilization via predictor-based design, we deal with a problem of a wave PDE coupled with an ODE in one boundary through a Neumann type interaction at the interface.
(3) This is the first contribution for the observer-based output-feedback stabilization of the coupled wave PDE-ODE system on a time-varying domain with the Neumann type interconnection.
(4) This is the first control design for the axial vibration suppression of the varying-length string with a payload, where the actuator acts at the boundary separated from the payload.

1.6 Notation. Throughout this paper, the partial derivatives and total derivatives are denoted as

Downloaded From: http://dynamicsystems.asmedigitalcollection.asme.org/ on 06/16/2018 Terms of Use: http://www.asme.org/about-asme/terms-of-use

$$f_x(x,t) = \frac{\partial f}{\partial x}(x,t), \quad f_t(x,t) = \frac{\partial f}{\partial t}(x,t)$$
$$\dot{f}(l(t),t) = \dot{l}(t) f_x(l(t),t) + f_t(l(t),t)$$
$$\beta'(x) = \frac{d\beta(x)}{dx}, \quad \dot{X}(t) = \frac{dX(t)}{dt}$$

2 Problem Formulation

A schematic of a mining cable elevator is depicted in Fig. 1. Because the catenary cable in Fig. 1(*a*) is much shorter than the vertical cable (comparing 70 m with 2000 m), we suppose that the vibrations on the catenary part are negligible, which gives the simplified model of a varying-length cable with a cage shown in Fig. 1(*b*). Due to the help of the lateral guides, the transverse vibrations in the vertical cable can be neglected since they are much smaller than the axial vibrations.

Two external forces are actuated. One is the motion control force $U_a(t)$ driven by a motor and the other is the vibration control force $U_v(t)$ manipulated by a hydraulic actuator at the floating sheave. The axial transport motion $z^*(t)$ is rigid-body motion neglecting the compliant property of the cable in the fixed coordinate system O', and $\dot{z}^*(t), \ddot{z}^*(t)$ are the velocity and acceleration accordingly. The dynamics of axial elastic deformations (vibration displacements) $u(x, t)$, with $u_t(x, t)$ being the vibration velocity accordingly, are referred to the moving coordinate system O associated with the motion $z^*(t)$. Here, we assume that the motion state $z^*(t)$ is controlled perfectly by the motion control force $U_a(t)$ and acts as the known target hosting trajectory. Then the axial vibration dynamics $u(x, t)$ on a prescribed time-varying domain $l(t) = L - z^*(t)$ is derived by Hamilton's principle [35] in the following.

2.1 Modeling of Physical System.

The kinetic energy E_k and the potential energy E_p of the system Fig. 1(*b*) are represented as

$$E_k = \frac{1}{2}\rho \int_0^{l(t)} \left(u_t(x,t) + \dot{z}^*(t)\right)^2 dx + \frac{1}{2} M\left(u_t(0,t) + \dot{z}^*(t)\right)^2 + \frac{1}{2}\frac{J_D}{R_D^2}\left(\dot{u}(l(t),t) + \dot{z}^*(t)\right)^2 \tag{1}$$

$$E_p = \frac{1}{2} E_A \int_0^{l(t)} u_x^2(x,t) dx + \int_0^{l(t)} T(x) u_x(x,t) dx + \rho g \int_0^{l(t)} \left(u(x,t) + z^*(t)\right) dx + Mg\left(u(0,t) + z^*(t)\right) \tag{2}$$

where $E_A = E \times A_a$ and $T(x) = (M + \rho x)g$ is the static tension in the cable.

The virtual work done by external forces is written as

$$\delta W = U_v(t)\delta(u(l(t),t) + z^*(t)) + c_1 \dot{u}(0,t)\delta u(0,t) + c_2(\dot{u}(l(t),t) + \dot{z}^*(t))\delta(u(l(t),t) + z^*(t)) \tag{3}$$

Substituting Eqs. (1)–(3) into extended Hamilton's principle

$$\int_{t_1}^{t_2} (\delta E_k - \delta E_p + \delta W) dt = 0 \tag{4}$$

and apply the variational operation. Note that because the length of the cable $l(t)$ changes with time, the domain of integration for the spatial variable is time-dependent. The standard procedure for integration by parts with respect to the temporal variable does not apply and some modifications are required. The use of Leibnitz's rule gives

$$\int_0^{l(t)} \rho\left(u_t(x,t) + \dot{z}^*(t)\right)\delta u_t dx = \frac{1}{dt}\int_0^{l(t)} \rho\left(u_t(x,t) + \dot{z}^*(t)\right)\delta u dx - \int_0^{l(t)} \rho\left(u_{tt}(x,t) + \ddot{z}^*(t)\right)\delta u dx - \dot{l}(t)\rho(u_t(l(t),t) + \dot{z}^*(t))\delta u(l(t),t) \tag{5}$$

Integrating Eq. (5) from t_1 to t_2 yields

$$\int_{t_1}^{t_2}\int_0^{l(t)} \rho(u_t(x,t) + \dot{z}^*(t))\delta u_t dx dt = -\int_{t_1}^{t_2}\int_0^{l(t)} \rho(u_{tt}(x,t) + \ddot{z}*(t))\delta u dx dt - \int_{t_1}^{t_2} \dot{l}(t)\rho(u_t(l(t),t) + \dot{z}^*(t))\delta u(l(t),t) dt \tag{6}$$

Applying Eq. (6) and following the standard procedure for integration by parts with respect to the spatial variable, one obtains from Eq. (4):

$$-\rho(u_{tt}(x,t) + \ddot{z}^*(t)) + E_A u_{xx}(x,t) - \rho g + T_x(x) = 0 \tag{7}$$

$$-M(u_{tt}(0,t) + \ddot{z}^*(t)) - Mg + T(0) + E_A u_x(0,t) + c_1 u_t(0,t) = 0 \tag{8}$$

$$U_v(t) - E_A u_x(l(t),t) - T(l(t)) - \dot{l}(t)\rho(u_t(l(t),t) + \dot{z}^*(t)) - \frac{J_D}{R_D^2}(\ddot{u}(l(t),t) + \ddot{z}^*(t)) + c_2(\dot{u}(l(t),t) + \dot{z}^*(t)) = 0 \tag{9}$$

Considering $T(x) = (M + \rho x)g$, we have the following relationships:

$$T(0) = Mg, \quad T_x(x) = \rho g \tag{10}$$

Inserting Eqs. (10), Eqs. (7)–(9) can be written as

$$-\rho(u_{tt}(x,t) + \ddot{z}^*(t)) + E_A u_{xx}(x,t) = 0 \tag{11}$$

$$-M(u_{tt}(0,t) + \ddot{z}^*(t)) + E_A u_x(0,t) + c_1 u_t(0,t) = 0 \tag{12}$$

$$U_v(t) - E_A u_x(l(t),t) - (M + \rho l(t))g - \dot{l}(t)\rho(u_t(l(t),t) + \dot{z}^*(t)) - \frac{J_D}{R_D^2}(\ddot{u}(l(t),t) + \ddot{z}^*(t)) + c_2(\dot{u}(l(t),t) + \dot{z}^*(t)) = 0 \tag{13}$$

2.2 Simplified Model for Controller Design.

In the controller design, we assume the acceleration of the target reference $\ddot{z}^*(t)$ is zero, which is reasonable because the velocity of the reference motion $z^*(t)$ can be set to be uniform except for starting and stopping moments in the practical operation of the elevator.

Remark 1. Although we derive the control design under the assumption $\ddot{z}^*(t) = 0$ in Eqs. (11)–(13), we conduct the simulation based on both the simplified model and the accurate model without the assumption $\ddot{z}^*(t) = 0$. The first one is to verify our theoretical result shown later about exponential stability of the output-feedback closed-loop system. The second one is to show that our control design is effective on vibration suppression of the mining cable elevator considered in this paper.

Then, the vibration dynamics Eqs. (11)–(13) can be written as

$$-\rho u_{tt}(x,t) + E_A u_{xx}(x,t) = 0 \tag{14}$$

$$-M u_{tt}(0,t) + E_A u_x(0,t) + c_1 u_t(0,t) = 0 \tag{15}$$

Downloaded From: http://dynamicsystems.asmedigitalcollection.asme.org/ on 06/16/2018 Terms of Use: http://www.asme.org/about-asme/terms-of-use

$$U_v(t) - E_A u_x(l(t),t) - (M+\rho l(t))g - \dot{l}(t)\rho(u_t(l(t),t)+\dot{z}^*(t)) - \frac{J_D}{R_D^2}\ddot{u}(l(t),t) + c_2(\dot{u}(l(t),t)+\dot{z}^*(t)) = 0 \quad (16)$$

Define the vibration control force as

$$U_v(t) = U_{v1}(t) + U_{v2}(t) \quad (17)$$

choosing $U_{v2}(t)$ as

$$U_{v2}(t) = (M+\rho l(t))g + \dot{l}(t)\rho(u_t(l(t),t)+\dot{z}^*(t)) + \frac{J_D}{R_D^2}\ddot{u}(l(t),t) - c_2(\dot{u}(l(t),t)+\dot{z}^*(t)) \quad (18)$$

Therefore, Eqs. (14)–(16) can be obtained as

$$\rho u_{tt}(x,t) = E_A u_{xx}(x,t), \quad \forall (x,t) \in [0,l(t)] \times [0,\infty) \quad (19)$$

$$-Mu_{tt}(0,t) + E_A u_x(0,t) + c_1 u_t(0,t) = 0 \quad (20)$$

$$U_{v1}(t) = E_A u_x(l(t),t) \quad (21)$$

2.3 Description in Coupled Partial Differential Equation-Ordinary Differential Equation System. The axial vibration dynamic system Eqs. (19)–(21) is a wave PDE with boundary conditions (21) and (20) described as a second-order ODE in time, which makes the problem difficult. To reduce the order of the boundary conditions, we introduce new variables $x_1(t)$ and $x_2(t)$ defined by

$$x_1(t) = u(0,t) \quad (22)$$

$$x_2(t) = u_t(0,t) \quad (23)$$

as the vibration displacement and the vibration velocity of the payload. Then, the following relation is obtained:

$$\dot{x}_1(t) = x_2(t) \quad (24)$$

$$\dot{x}_2(t) = -\frac{E_A}{M}u_x(0,t) - \frac{c_1}{M}u_t(0,t) \quad (25)$$

Let $X(t) \in \mathbb{R}^{2\times 1}$ be a state variable defined by

$$X(t) = [x_1(t), x_2(t)]^{\mathrm{T}} \quad (26)$$

Through the definition Eq. (26), we rewrite Eqs. (19)–(21) as the following coupled PDE-ODE system:

$$\dot{X}(t) = AX(t) + Bu_x(0,t) \quad (27)$$

$$u(0,t) = \mathrm{C}X(t) \quad (28)$$

$$u_{tt}(x,t) = \frac{E_A}{\rho}u_{xx}(x,t) \quad (29)$$

$$E_A u_x(l(t),t) = U_{v1}(t) \quad (30)$$

where

$$A = \begin{bmatrix} 0 & 1 \\ 0 & \frac{-c_1}{M} \end{bmatrix}, \quad B = \frac{E_A}{M}\begin{bmatrix} 0 \\ -1 \end{bmatrix}, \quad C = [1, 0] \quad (31)$$

The Neumann interconnection in ODE Eq. (27) physically amounts to the force acting on the cage.

Remark 2. The cage-guide boundary is damped when the damping coefficients $c_1 > 0$ in Eq. (8). We process the control design based on a more general model where c_1 is arbitrary. It means the uncontrolled boundary in the wave equation can be damped ($c_1 > 0$), undamped ($c_1 = 0$), or even anti-damped ($c_1 < 0$).

The more general wave PDE-ODE model is considered in the control design as

$$\dot{X}(t) = AX(t) + Bu_x(0,t) \quad (32)$$

$$u_{tt}(x,t) = qu_{xx}(x,t) \quad (33)$$

$$u(0,t) = \mathrm{C}X(t) \quad (34)$$

$$u_x(l(t),t) = U(t) \quad (35)$$

$\forall (x,t) \in [0,l(t)] \times [0,\infty)$, where q is an arbitrary positive constant. $A \in \mathbb{R}^{2\times 2}$, $B \in \mathbb{R}^{2\times 1}$, $C \in \mathbb{R}^{1\times 2}$ satisfy that the pair $[A, B]$ is controllable and pair $[A, C]$ is observable and $CB = 0$. $X(t) \in \mathbb{R}^2$ is the ODE state and $u(x, t) \in R$ is the state of the wave PDE. $U(t) = 1/E_A U_{v1}(t)$ is the control input to be designed.

Remark 3. Our control design is also applicable to other physical problems described by the wave PDE-stable/unstable/antistable ODE coupled model, such as controlling the torsional vibration dynamics of drill strings with stick-slip instabilities arising in deep oil drilling [36].

In the control design of this paper, the time-varying spatial domain $l(t)$ is assumed to have following properties, which are reasonable for the string's length of the ascending mining cable elevator:

Assumption 1. *There exists a lower bound* $\underline{l} > 0$, *s.t.* $l(t) \geq \underline{l}$, $\forall t \geq 0$.

Assumption 2. *The domain length l(t) of the wave PDE is decreasing,* i.e., $\dot{l}(t) \leq 0$.

3 State-Feedback Control Design

In this section, we design the state-feedback controller, which stabilizes the systems (32)–(35) with the full-state measurements $u(x, t)$ for $\forall x \in [0, l(t)]$ and $X(t)$. We seek an invertible transformation that converts the (X, u)-system into the following stable target system (X, w), described as:

$$\dot{X}(t) = (A+BK)X(t) + Bw_x(0,t) \quad (36)$$

$$w_{tt}(x,t) = qw_{xx}(x,t) \quad (37)$$

$$w(0,t) = 0 \quad (38)$$

$$w_x(l(t),t) = -dw_t(l(t),t) \quad (39)$$

where $d > 0$ is a positive arbitrary damping gain. K is chosen to make $A + BK$ Hurwitz. Based on Refs. [25] and [37], the backstepping transformation is formulated as

$$w(x,t) = u(x,t) - \int_0^x \gamma(x,y)u(y,t)dy - \int_0^x h(x,y)u_t(y,t)dy - \beta(x)X(t) \quad (40)$$

where the kernel functions $\gamma(x, y) \in R$, $h(x, y) \in R$, and $\beta(x) \in \mathbb{R}^{1\times 2}$ are to be determined. Taking second derivatives of Eq. (40) with respect to x and t, respectively, along the solution of Eqs. (32)–(35), we have

Downloaded From: http://dynamicsystems.asmedigitalcollection.asme.org/ on 06/16/2018 Terms of Use: http://www.asme.org/about-asme/terms-of-use

$$
\begin{aligned}
&w_{tt}(x,t)-qw_{xx}(x,t)\\
&=2q\left(\frac{d}{dx}\gamma(x,x)\right)u(x,t)\\
&\quad+q\int_0^x\big(h_{xx}(x,y)-h_{yy}(x,y)\big)u_t(y,t)dy\\
&\quad+q\int_0^x(\gamma_{xx}(x,y)-\gamma_{yy}(x,y))u(y,t)dy\\
&\quad+2q\left(\frac{d}{dx}h(x,x)\right)u_t(x,t)\\
&\quad-\big(\beta(x)AB-q\gamma(x,0)+qh_y(x,0)CB\big)u_x(0,t)\\
&\quad+\big(qh(x,0)-\beta(x)B\big)u_{xt}(0,t)\\
&\quad+\Big(q\beta''(x)-\beta(x)A^2-q\gamma_y(x,0)C-qh_y(x,0)CA\Big)X(t)=0
\end{aligned}
\tag{41}
$$

For Eq. (41) to hold, the following conditions must be satisfied:

$$\frac{d}{dx}\gamma(x,x)=0 \tag{42}$$

$$\gamma_{xx}(x,y)=\gamma_{yy}(x,y), \tag{43}$$

$$\frac{d}{dx}h(x,x)=0, \tag{44}$$

$$h_{xx}(x,y)=h_{yy}(x,y) \tag{45}$$

$$qh(x,0)=\beta(x)B \tag{46}$$

$$\beta(x)AB=q\gamma(x,0)-qh_y(x,0)CB \tag{47}$$

$$q\beta''(x)=\beta(x)A^2+q\gamma_y(x,0)C+qh_y(x,0)CA \tag{48}$$

Substituting the transformation Eq. (40) into Eqs. (36) and (38), and comparing them with Eqs. (32) and (34), we can chose $\beta(x)$ to satisfy

$$\beta'(0)=K-\gamma(0,0)C-h(0,0)CA \tag{49}$$

$$\beta(0)=C \tag{50}$$

By conditions Eqs. (42)–(45), $\gamma(x, y)$ and $h(x, y)$ can be written as

$$\gamma(x,y)=m(x-y) \tag{51}$$

$$h(x,y)=n(x-y) \tag{52}$$

Let $D\in\mathbb{R}^{4\times4}$ and $\Lambda\in\mathbb{R}^{1\times2}$ be defined as

$$D=\begin{bmatrix}0 & \frac{1}{q}A^2\\ I & -\frac{1}{q}(BCA+ABC)\end{bmatrix} \tag{53}$$

$$\Lambda=\frac{1}{q}\mathrm{C}ABC \tag{54}$$

Solving Eqs. (46)–(50) with the help of Eqs. (51) and (52), the explicit solutions of $\beta(x)$, $\gamma(x, y)$, and $h(x, y)$ are obtained as

$$\beta(x)=[C,\quad K-\Lambda]e^{Dx}\begin{bmatrix}I\\0\end{bmatrix} \tag{55}$$

$$\gamma(x,y)=\frac{1}{q}\beta(x-y)AB \tag{56}$$

$$h(x,y)=\frac{1}{q}\beta(x-y)B \tag{57}$$

where $I\in\mathbb{R}^{2\times2}$ is an identity matrix. For the mining elevator modeled in Sec. 2, the solutions of gain kernels (55)–(57) are written as

$$\beta(x)=-\frac{M}{\rho}\left[k_1-\left(k_1+\frac{\rho}{M}\right)e^{\frac{\rho}{M}x},k_2-k_2e^{\frac{\rho}{M}x}\right] \tag{58}$$

$$\gamma(x,y)=k_1-\left(k_1+\frac{\rho}{M}\right)e^{\frac{\rho}{M}(x-y)} \tag{59}$$

$$h(x,y)=k_2-k_2e^{\frac{\rho}{M}(x-y)} \tag{60}$$

where $k_1>0$, $k_2>0$ are controller gains such that $K=[k_1,\ k_2]$ makes $(A+BK)$ Hurwitz. For the boundary Eq. (39) to hold, the state-feedback control law is given by

$$
\begin{aligned}
U(t)=\frac{1}{N_1}\Bigg(&N_2u_t(l(t),t)+N_3u(l(t),t)\\
&+N_4u_x(0,t)+N_5u(0,t)+N_6X(t)\\
&+\int_0^{l(t)}N_7u(x,t)dx+\int_0^{l(t)}N_8u_t(x,t)dx\Bigg)
\end{aligned}
\tag{61}
$$

where

$$N_1=1-dKB \tag{62}$$

$$N_2=-d \tag{63}$$

$$N_3(l(t))=\gamma(l(t),l(t))-qh_{xy}(l(t),l(t)) \tag{64}$$

$$N_4(l(t))=dqh_x(l(t),0)-d\beta(l(t))B \tag{65}$$

$$N_5(l(t))=qdh_{xy}(l(t),0) \tag{66}$$

$$N_6(l(t))=\beta_x(l(t))+d\beta(l(t))A \tag{67}$$

$$N_7(l(t),x)=\gamma_x(l(t),x)+qh_{xyy}(l(t),x) \tag{68}$$

$$N_8(l(t),x)=h_x(l(t),x)+d\gamma(l(t),x) \tag{69}$$

In the same manner to obtain the direct transformation, we also obtain the inverse transformation

$$
\begin{aligned}
u(x,t)=w(x,t)&-\int_0^x\varphi(x,y)w(y,t)dy\\
&-\int_0^x\lambda(x,y)w_t(y,t)dy-\alpha(x)X(t)
\end{aligned}
\tag{70}
$$

with

$$\alpha(x)=[-C\quad -K]e^{Zx}\begin{bmatrix}I\\0\end{bmatrix} \tag{71}$$

$$\varphi(x,y)=\frac{1}{q}\alpha(x-y)(A+BK)B \tag{72}$$

$$\lambda(x,y)=\frac{1}{q}\alpha(x-y)B \tag{73}$$

Downloaded From: http://dynamicsystems.asmedigitalcollection.asme.org/ on 06/16/2018 Terms of Use: http://www.asme.org/about-asme/terms-of-use

where

$$Z = \begin{bmatrix} 0 & q(A+BK)^2 \\ I & 0 \end{bmatrix} \quad (74)$$

The detailed procedure to derive the inverse transformation (70) is shown in the Appendix.

4 Observer and Output-Feedback Control Design

In Sec. 3, a state-feedback controller is designed to stabilize the original system exponentially. However, the designed state-feedback control law requires an infinite number of sensors to obtain the distributed states in a whole domain, which is not feasible in practice. In this section, we propose an observer-based output feedback control law, which requires only a few boundary values as available measurements. An exponentially convergent observer is designed to reconstruct the distributed states using a finite number of available boundary measurements in Sec. 4.1 and the output feedback control law based on the observer is proposed in Sec. 4.2. Suppose the available measurement of the system is $X(t)$, which is not collocated with the actuator. In the mining cable elevator, the acceleration sensor placed at the cage with the integration algorithm can be used to obtain $X(t) = [u(0,\ t),\ u_t(0,\ t)]$. Here, the initial condition of the vibration displacement at the cage can be obtained by the static equilibrium equation and the initial velocity is zero.

4.1 Observer Design. The observer structure consists of a copy of the plant (32)–(35) plus the boundary state error injection, described as

$$\dot{\hat{X}}(t) = A\hat{X}(t) + B\hat{u}_x(0,t) + \bar{L}C(X(t) - \hat{X}(t)) \quad (75)$$

$$\hat{u}_{tt}(x,t) = q\hat{u}_{xx}(x,t) - D_1(X(t) - \hat{X}(t)) \quad (76)$$

$$\hat{u}(0,t) = CX(t) - D_2(X(t) - \hat{X}(t)) \quad (77)$$

$$\hat{u}_x(l(t),t) = U(t) \quad (78)$$

The observer gains D_1, D_2, and $\bar{L} = [\bar{l}_1, \bar{l}_2]^{\mathrm{T}}$ are to be determined. Define the observer errors as

$$\tilde{u}(x,t) = u(x,t) - \hat{u}(x,t) \quad (79)$$

$$\tilde{X}(t) = X(t) - \hat{X}(t) \quad (80)$$

Then, subtracting Eqs. (75)–(78) from Eqs. (32)–(35) provides the observer error system written as

$$\dot{\tilde{X}}(t) = (A - \bar{L}C)\tilde{X}(t) + B\tilde{u}_x(0,t) \quad (81)$$

$$\tilde{u}_{tt}(x,t) = q\tilde{u}_{xx}(x,t) + D_1\tilde{X}(t) \quad (82)$$

$$\tilde{u}(0,t) = D_2\tilde{X}(t) \quad (83)$$

$$\tilde{u}_x(l(t),t) = 0 \quad (84)$$

To convert the systems (81)–(84) into the following exponentially stable target system described as:

$$\dot{\tilde{X}}(t) = (A - \bar{L}C)\tilde{X}(t) + B\tilde{w}_x(0,t) \quad (85)$$

$$\tilde{w}_{tt}(x,t) = q\tilde{w}_{xx}(x,t) \quad (86)$$

$$\tilde{w}(0,t) = 0 \quad (87)$$

$$\tilde{w}_x(l(t),t) = -\bar{d}\tilde{w}_t(l(t),t) \quad (88)$$

where $\bar{L}$ is chosen to make $A - \bar{L}C$ Hurwitz and $\bar{d}$ is an arbitrary positive design parameter, the following direct and inverse transformations are formulated:

$$\tilde{u}(x,t) = \tilde{w}(x,t) - \int_0^x d_0(x,y)\tilde{w}(y,t)dy - \int_0^x d_1(x,y)\tilde{w}_t(y,t)dy - \Gamma(x)\tilde{X}(t) \quad (89)$$

$$\tilde{w}(x,t) = \tilde{u}(x,t) - \int_0^x d_2(x,y)\tilde{u}(y,t)dy - \int_0^x d_3(x,y)\tilde{u}_t(y,t)dy - \psi(x)\tilde{X}(t) \quad (90)$$

By matching Eqs. (81)–(84) and Eqs. (85)–(88), the following conditions are obtained:

$$\Gamma(x)AB = qd_0(x,0) \quad (91)$$

$$qd_1(x,0) = \Gamma(x)B \quad (92)$$

$$q\Gamma''(x) = \Gamma(x)(A - \bar{L}C)^2 + D_1 \quad (93)$$

$$D_2 = -\Gamma(0) \quad (94)$$

$$\Gamma'(0) = 0 \quad (95)$$

$$d_1(l(t),l(t)) = -\bar{d} \quad (96)$$

$$d_0(l(t),l(t)) = 0 \quad (97)$$

$$d_{0x}(l(t),y) = 0 \quad (98)$$

$$d_{1x}(l(t),y) = 0 \quad (99)$$

The solutions of the gain kernels in Eq. (89) are obtained as

$$\Gamma(x) = -[0, q\bar{d}][AB, B]^{-1} \quad (100)$$

$$d_0(x,y) = 0 \quad (101)$$

$$d_1(x,y) = -\bar{d} \quad (102)$$

The observer gains are obtained as

$$D_1 = [0, q\bar{d}][AB, B]^{-1}(A - \bar{L}C)^2 \quad (103)$$

$$D_2 = [0, q\bar{d}][AB, B]^{-1} \quad (104)$$

Here, the matrix $[AB,\ B]$ is invertible since the pair $[A,\ B]$ is controllable.

For the mining elevator modeled in Sec. 2, the solutions of the gain kernels (100)–(102) are written as

$$\Gamma = \left[\frac{c_1\bar{d}}{\rho}, \frac{M\bar{d}}{\rho}\right] \quad (105)$$

$$d_0 = 0 \quad (106)$$

$$d_1 = -\bar{d} \quad (107)$$

and then the observer gains Eqs. (103) and (104) are obtained as

Downloaded From: http://dynamicsystems.asmedigitalcollection.asme.org/ on 06/16/2018 Terms of Use: http://www.asme.org/about-asme/terms-of-use

$$D_1 = -\frac{\overline{d}}{\rho}\left[c_1\left(\overline{l}_1^2 - \overline{l}_2\right) + M\left(l_1 l_2 + \frac{c_1 l_2}{M}\right) - c_1\left(\frac{c_1}{M} + l_1\right) + M\left(\frac{c_1^2}{M^2} - l_2\right)\right] \quad (108)$$

$$D_2 = \left[-\frac{c_1\overline{d}}{\rho}, -\frac{M\overline{d}}{\rho}\right] \quad (109)$$

$A - \overline{L}C$ can be Hurwitz by choosing positive parameters $\overline{l}_1 > 0$ and $\overline{l}_2 > 0$.

4.2 Output-Feedback Control Design. To design the output-feedback controller, we consider the target $(\hat{X}, \hat{w})$-subsystem, which is constructed by the direct and inverse transformations with the same gain kernels as the state feedback Eqs. (40) and (70). Hence, we introduce the following transformations from $(\hat{X}, \hat{u})$ to $(\hat{X}, \hat{w})$ described as:

$$\hat{w}(x,t) = \hat{u}(x,t) - \int_0^x \gamma(x,y)\hat{u}(y,t)dy - \int_0^x h(x,y)\hat{u}_t(y,t)dy - \beta(x)\hat{X}(t) \quad (110)$$

$$\hat{u}(x,t) = \hat{w}(x,t) - \int_0^x \varphi(x,y)\hat{w}(y,t)dy - \int_0^x \lambda(x,y)\hat{w}_t(y,t)dy - \alpha(x)\hat{X}(t) \quad (111)$$

Taking time and spatial derivatives of Eq. (110) with the help of gain kernels (55)–(57) and $(\hat{X}, \hat{u})$-system (75)–(78), we derive the following coupled PDE-ODE $(\hat{X}, \hat{w})$-system:

$$\dot{\hat{X}}(t) = (A + BK)\hat{X}(t) + B\hat{w}_x(0,t) + (\overline{L}C + B\gamma(0,0)(C - D_2))\tilde{X}(t) \quad (112)$$

$$\hat{w}_{tt}(x,t) = q\hat{w}_{xx}(x,t) - f_1(x)\tilde{X}(t) - f_2(x)\tilde{w}_x(0,t) \quad (113)$$

$$\hat{w}(0,t) = (C - D_2)\tilde{X}(t) \quad (114)$$

$$\hat{w}_x(l(t),t) = -d\hat{w}_t(l(t),t) \quad (115)$$

where

$$f_1(x) = \beta(x)A\overline{L}C + \beta(x)\overline{L}C(A - \overline{L}C) - \int_0^x h(x,y)D_1(A - \overline{L}C)dy - \int_0^x \gamma(x,y)D_1 dy \quad (116)$$

$$f_2(x) = -\int_0^x h(x,y)D_1 B dy + \beta(x)\overline{L}CB \quad (117)$$

By Eq. (115), the output-feedback control law is designed as

$$U(t) = \frac{1}{N_1}\Bigg(N_2\hat{u}_t(l(t),t) + N_3\hat{u}(l(t),t) + N_4(l(t))\hat{u}_x(0,t) + N_5(l(t))\hat{u}(0,t) + N_6(l(t))\hat{X}(t) + \int_0^{l(t)} N_7(l(t),x)\hat{u}(x,t)dx + \int_0^{l(t)} N_8(l(t),x)\hat{u}_t(x,t)dx\Bigg) \quad (118)$$

Remark 4. If time delay is considered, two ways can be used to accommodate the delay: one is by incorporating damping into the model and performing control design for that model, as was done in Refs. [38] and [39]. Another one is compensating a known time delay at the input to a wave equation, as described in Ref. [40].

5 Stability Analysis

In this section, we establish the stability proof of the target system via Lyapunov analysis of PDEs. The equivalent stability property between the target system and the original system is ensured due to the invertibility of the backstepping transformation. The main theorem of this paper is stated in the following.

THEOREM 1. *For any initial estimates $(\hat{u}(x,0), \hat{X}(0))$ compatible with the control law (118) and initial values $(u(x,0), u_t(x,0))$, which belong to $H^1(0,L) \times L^2(0,L)$, the closed-loop system consisting of the plant (32)–(35) and the observer design (75)–(78) with the output-feedback control law (118) is exponentially stable in the sense of the norm*

$$\left(\int_0^{l(t)} u_t^2(x,t)dx + \int_0^{l(t)} u_x^2(x,t)dx + \int_0^{l(t)} \hat{u}_t^2(x,t)dx + \int_0^{l(t)} \hat{u}_x^2(x,t)dx + |X(t)|^2 + |\hat{X}(t)|^2\right)^{1/2} \quad (119)$$

Proof. First, we show the stability of $(\tilde{X}, \tilde{w})$-subsystem. Define

$$\Omega_1(t) = \|\tilde{u}_t(t)\|^2 + \|\tilde{u}_x(t)\|^2 + |\tilde{X}(t)|^2 \quad (120)$$

$$\Xi_1(t) = \|\tilde{w}_t(t)\|^2 + \|\tilde{w}_x(t)\|^2 + |\tilde{X}(t)|^2 \quad (121)$$

where $\|\tilde{u}(t)\|^2$ is a compact notation for $\int_0^{l(t)} \tilde{u}(x,t)^2 dx$. In addition, we employ a Lyapunov function

$$V_1 = \tilde{X}^{\mathrm{T}}(t)P_1\tilde{X}(t) + \phi_1 E_1(t) \quad (122)$$

where the matrix $P_1 = P_1^{\mathrm{T}} > 0$ is the solution to the Lyapunov equation

$$P_1(A - \overline{L}C) + (A - \overline{L}C)^{\mathrm{T}}P_1 = -Q_1 \quad (123)$$

for some $Q_1 = Q_1^{\mathrm{T}} > 0$. The positive parameter ϕ_1 is to be chosen later. $E_1(t)$ is defined as

$$E_1(t) = \frac{1}{2}\|\tilde{w}_t(t)\|^2 + \frac{q}{2}\|\tilde{w}_x(t)\|^2 + \delta_1\int_0^{l(t)} (1+x)\tilde{w}_x(x,t)\tilde{w}_t(x,t)dx \quad (124)$$

where the parameter δ_1 should satisfy

$$0 < \delta_1 < \frac{1}{1+L}\min\{1, q\} \quad (125)$$

Then, we get

$$\theta_{11}\Xi_1(t) \le V_1(t) \le \theta_{12}\Xi_1(t) \quad (126)$$

where

$$\theta_{11} = \min\left\{\lambda_{\min}(P_1), \frac{\phi_1}{2}(1 - \delta_1(1+L)), \frac{\phi_1}{2}(q - \delta_1(1+L))\right\} > 0 \quad (127)$$

Downloaded From: http://dynamicsystems.asmedigitalcollection.asme.org/ on 06/16/2018 Terms of Use: http://www.asme.org/about-asme/terms-of-use

$$\theta_{12} = \max\left\{\lambda_{\max}(P_1), \frac{\phi_1}{2}(1+\delta_1(1+L)), \frac{\phi_1}{2}(q+\delta_1(1+L))\right\} > 0 \quad (128)$$

Time derivative of V_1 along Eqs. (85)–(88) is obtained as

$$\begin{aligned}\dot{V}_1 = & -\bar{d}q\phi_1\tilde{w}_t^2(l(t),t) - \frac{1}{2}|\dot{l}(t)|\phi_1\tilde{w}_t^2(l(t),t) \\ & - \frac{q}{2}|\dot{l}(t)|\phi_1\tilde{w}_x^2(l(t),t) - \tilde{X}^T(t)Q_1\tilde{X}(t) \\ & + 2BP_1\tilde{w}_x(0,t)\tilde{X}(t) + \frac{\delta_2}{2}(1+l(t))\phi_1\tilde{w}_t^2(l(t),t) \\ & + q\bar{d}^2\frac{\delta_1}{2}(1+l(t))\phi_1\tilde{w}_t^2(l(t),t) \\ & - q\frac{\delta_1}{2}\phi_1\tilde{w}_x^2(0,t) - \frac{\delta_1}{2}\phi_1\|\tilde{w}_t\|^2 - \frac{\delta_1}{2}q\phi_1\|\tilde{w}_x\|^2 \\ & + |\dot{l}(t)|\bar{d}\delta_1(1+l(t))\phi_1\tilde{w}_t^2(l(t),t) \end{aligned} \quad (129)$$

Remark 5. Assumption 2 yields $\dot{l}(t) = -|\dot{l}(t)|$.

Applying Young's inequality to Eq. (129), the following inequality is obtained:

$$\begin{aligned}\dot{V}_1 \le & -\frac{1}{2}\lambda_{\min}(Q_1)|\tilde{X}(t)|^2 - \frac{\delta_1}{2}\phi_1\|\tilde{w}_t\|^2 - \frac{\delta_1}{2}q\phi_1\|\tilde{w}_x\|^2 \\ & - \left(\bar{d}q - \frac{\delta_1(1+L)}{2}\left(1+q\bar{d}^2\right)\right)\phi_1\tilde{w}_t^2(l(t),t) \\ & - |\dot{l}(t)|\left(\frac{1}{2}+\frac{\bar{d}^2q}{2} - \bar{d}\delta_1(1+L)\right)\phi_1\tilde{w}_t(l(t),t)^2 \\ & - \left(q\frac{\delta_1}{2}\phi_1 - \frac{2|P_1B|^2}{\lambda_{\min}(Q_1)}\right)\tilde{w}_x(0,t)^2 \end{aligned} \quad (130)$$

Therefore, combining with Eq. (125), the parameter δ_1 and ϕ_1 are chosen to satisfy the following:

$$0 < \delta_1 < \frac{1}{1+L}\min\left\{1, q, \frac{2\bar{d}q}{1+q\bar{d}^2}, \frac{1+q\bar{d}^2}{2\bar{d}}\right\} \quad (131)$$

$$\phi_1 > \frac{4|P_1B|^2}{q\delta_1\lambda_{\min}(Q_1)} + \varpi \quad (132)$$

with a positive parameter ϖ. Then, we arrive at

$$\dot{V}_1 \le -\sigma_1V_1 - \varpi\tilde{w}_x(0,t)^2 \le -\sigma_1V_1 \quad (133)$$

where

$$\sigma_1 = \frac{1}{\theta_{12}}\min\left\{\frac{\delta_1}{2}\phi_1, \frac{\delta_1}{2}q\phi_1, \frac{1}{2}\lambda_{\min}(Q_1)\right\} \quad (134)$$

Next, we show the stability analysis of the $(\hat{X},\hat{w})$-subsystem. Define

$$\Omega_2(t) = \|\hat{u}_t(t)\|^2 + \|\hat{u}_x(t)\|^2 + |\hat{X}(t)|^2 \quad (135)$$

$$\Xi_2(t) = \|\hat{w}_t(t)\|^2 + \|\hat{w}_x(t)\|^2 + |\hat{X}(t)|^2 \quad (136)$$

Let V_2 be a Lyapunov function written as

$$V_2 = \hat{X}^{\mathrm{T}}(t)P_2\hat{X}(t) + \phi_2E_2(t) \quad (137)$$

where the matrix $P_2 = P_2^{\mathrm{T}} > 0$ is the solution to the following Lyapunov equation:

$$P_2(A+BK) + (A+BK)^{\mathrm{T}}P_2 = -Q_2 \quad (138)$$

for some $Q_2 = Q_2^{\mathrm{T}} > 0$. The positive parameter ϕ_2 is to be chosen later. Define $E_2(t)$ as

$$E_2(t) = \frac{1}{2}\|\hat{w}_t(t)\|^2 + \frac{q}{2}\|\hat{w}_x(t)\|^2 + \delta_2\int_0^{l(t)}(1+x)\hat{w}_x(x,t)\hat{w}_t(x,t)dx \quad (139)$$

the parameter δ_2 must be chosen to satisfy

$$0 < \delta_2 < \frac{1}{1+L}\min\{1, q\} \quad (140)$$

Similar with Eqs. (126)–(128), we get

$$\theta_{21}\Xi_2(t) \le V_2(t) \le \theta_{22}\Xi_2(t) \quad (141)$$

where

$$\theta_{21} = \min\left\{\lambda_{\min}(P_2), \frac{\phi_2}{2}(1-\delta_2(1+L)),\ \frac{\phi_2}{2}(q-\delta_2(1+L))\right\} > 0 \quad (142)$$

$$\theta_{22} = \max\left\{\lambda_{\max}(P_2), \frac{\phi_2}{2}(1+\delta_2(1+L)),\ \frac{\phi_2}{2}(q+\delta_2(1+L))\right\} > 0 \quad (143)$$

Taking the time derivative of V_2 along Eqs. (112)–(115), we get

$$\begin{aligned}\dot{V}_2 = & \phi_2q\int_0^{l(t)}\hat{w}_t(x,t)\hat{w}_{xx}(x,t)dx \\ & + \phi_2q\int_0^{l(t)}\hat{w}_x(x,t)\hat{w}_{xt}(x,t)dx \\ & - \phi_2\int_0^{l(t)}\hat{w}_t(x,t)\left[f_1(x)\tilde{X}(t) + f_2(x)\tilde{w}_x(0,t)\right]dx \\ & - \phi_2|\dot{l}(t)|\frac{1}{2}\hat{w}_t^2(l(t),t) - q\phi_2|\dot{l}(t)|\frac{1}{2}\hat{w}_x^2(l(t),t) \\ & + \frac{1}{2}\phi_2q\delta_2(1+l(t))\hat{w}_x^2(l(t),t) - \frac{1}{2}\phi_2q\delta_2\hat{w}_x^2(0,t) \\ & - \frac{1}{2}\phi_2q\delta_2\|\hat{w}_x\|^2 + \frac{1}{2}\phi_2\delta_2(1+l(t))\hat{w}_t^2(l(t),t) \\ & - \frac{1}{2}\phi_2\delta_2\hat{w}_t^2(0,t) - \frac{1}{2}\phi_2\delta_2\|\hat{w}_t\|^2 \\ & + \phi_2\dot{l}(t)\delta_2(1+l(t))\hat{w}_t(l(t),t)\hat{w}_x(l(t),t) \\ & + \dot{\hat{X}}^{\mathrm{T}}(t)P_2\hat{X}(t) + \hat{X}^{\mathrm{T}}(t)P_2\dot{\hat{X}}(t) \end{aligned} \quad (144)$$

Applying Young's inequality to Eq. (144) as in Eq. (130), the following inequality is obtained:

Downloaded From: http://dynamicsystems.asmedigitalcollection.asme.org/ on 06/16/2018 Terms of Use: http://www.asme.org/about-asme/terms-of-use

$$\dot{V}_2 \le -\left(\frac{1}{2}\phi_2\delta_2 - (B_1+B_2)L\right)\|\hat{w}_t\|^2 - \frac{1}{2}q\phi_2\delta_2\|\hat{w}_x\|^2 - \frac{1}{2}\lambda_{\min}(Q_2)|\tilde{X}(t)|^2 - \left(\frac{1}{2}q\phi_2\delta_2 - \frac{1}{2}q^2 - \frac{4|P_2B|^2}{\lambda_{\min}(Q_2)}\right)\hat{w}_x^2(0,t) - \phi_2\left(qd - \frac{\delta_2}{2}(1+L)(1+qd^2)\right)\hat{w}_t(l(t),t)^2 - \phi_2|\dot{l}(t)|\left(\frac{1}{2}+\frac{qd^2}{2} - d\delta_2(1+L)\right)\hat{w}_t(l(t),t)^2 + \left(\frac{1}{4}\phi_2^2 + \frac{1}{2}\phi_2^2(C-D_2)^2(A-\overline{L}C)^2 + \frac{4|P_2(\overline{L}C + B\gamma(0,0)(C-D_2))|^2}{\lambda_{\min}(Q_2)}\right)|\tilde{X}(t)|^2 + \frac{1}{4}\phi_2^2\tilde{w}_x^2(0,t) \quad (145)$$

where B_i for $i = 1, 2$ are defined as

$$B_i = \max_{x\in[0,L]}\{|f_i(x)|^2\}$$

Therefore, by choosing the parameter δ_2 and ϕ_2 as

$$0 < \delta_2 < \frac{1}{1+L}\min\left\{1, q, \frac{2dq}{1+qd^2}, \frac{1+qd^2}{2d}\right\} \quad (146)$$

$$\phi_2 = \frac{2}{\delta_2}\max\left\{2(B_1+B_2)L, \frac{q}{2} + \frac{4|P_2B|^2}{q\lambda_{\min}(Q_2)}\right\} \quad (147)$$

we arrive at

$$\dot{V}_2 \le -\sigma_2 V_2 + \xi_1|\tilde{X}(t)|^2 + \xi_2\tilde{w}_x^2(0,t) \quad (148)$$

where $\sigma_2 = \mu_2/\theta_{22} > 0$, and

$$\mu_2 = \min\left\{\frac{1}{4}\phi_2\delta_2, \frac{1}{2}q\phi_2\delta_2, \frac{1}{2}\lambda_{\min}(Q_2)\right\} \quad (149)$$

$$\xi_1 = \frac{1}{4}\phi_2^2 + \frac{1}{2}\phi_2^2(C-D_2)^2(A-\overline{L}C)^2 + \frac{4|P_2(\overline{L}C + B\gamma(0,0)(C-D_2))|^2}{\lambda_{\min}(Q_2)} \quad (150)$$

$$\xi_2 = \frac{1}{4}\phi_2^2 \quad (151)$$

Let V be the Lyapunov function of the overall $(\tilde{X}, \tilde{w}, \hat{X}, \hat{w})$-system defined as

$$V = RV_1 + V_2 \quad (152)$$

Taking time derivative of Eq. (152) and using Eqs. (126), (133), and (148), we get

$$\dot{V} \le -\frac{R\sigma_1}{2}V_1 - \sigma_2V_2 - \left(\frac{R\sigma_1\theta_{12}}{2} - \xi_1\right)|\tilde{X}(t)|^2 - (R\varpi - \xi_2)\tilde{w}_x(0,t)^2 \quad (153)$$

Therefore, choosing R sufficiently large, finally we arrive at

$$\dot{V} \le -\sigma V \quad (154)$$

for some positive σ. The differential inequality Eq. (154) deduces that there exists a positive parameter $\eta_1 > 0$ such that

$$\|\tilde{w}_t\|^2 + \|\tilde{w}_x\|^2 + |\tilde{X}(t)|^2 + \|\hat{w}_t\|^2 + \|\hat{w}_x\|^2 + |\hat{X}(t)|^2 \le \eta_1(\|\tilde{w}_t(0)\|^2 + \|\tilde{w}_x(0)\|^2 + |\tilde{X}(0)|^2 + \|\hat{w}_t(0)\|^2 + \|\hat{w}_x(0)\|^2 + |\hat{X}(0)|^2)e^{-\sigma t} \quad (155)$$

Therefore, the overall target system $(\tilde{w}, \tilde{X}, \hat{w}, \hat{X})$ is exponentially stable. Due to the invertibility of the transformations Eqs. (90) and (110) as explicitly written in Eqs. (89) and (111), applying Poincare's, Young's, and Cauchy–Schwartz inequalities to Eq. (155) in a similar manner as Theorem 16.1 in Ref. [37] yields

$$\|\tilde{u}_t\|^2 + \|\tilde{u}_x\|^2 + |\tilde{X}(t)|^2 + \|\hat{u}_t\|^2 + \|\hat{u}_x\|^2 + |\hat{X}(t)|^2 \le \eta_2(\|\tilde{u}_t(0)\|^2 + \|\tilde{u}_x(0)\|^2 + |\tilde{X}(0)|^2 + \|\hat{u}_t(0)\|^2 + \|\hat{u}_x(0)\|^2 + |\hat{X}(0)|^2)e^{-\sigma t} \quad (156)$$

for some positive η_2. Therefore, the exponential stability of the overall original system $(\tilde{u}, \tilde{X}, \hat{u}, \hat{X})$ in the sense of Eqs. (120) and (135) is proved, which concludes Theorem 1 with the help of Eqs. (79) and (80).

6 Numerical Simulation

The simulation is performed based on the simplified model and the accurate model. In detail, in the first case, the simplified model (27)–(30) under the designed state-feedback control law (61) and the output-feedback control law (118) is conducted to verify the theoretical result in Theorem 1. In the second case, the accurate model (11)–(13) with Eq. (18) under the designed output-feedback control law (118) is used to test the controller performance on vibration suppression. Note that the control input U_{v1} applied in both cases is $U_{v1} = E_AU(t)$ where $U(t)$ is the designed control law and the constant $E_A = E \times A_a$.

The physical parameters of the mining cable elevator used in the simulation are shown in Table 1. To highlight the controller performance on vibration suppression, we make the damping coefficient c_1 in the elevator be zero. The designed reference of the hoisting velocity $\dot{z}^*(t) = \dot{l}(t)$ is plotted in Fig. 2. The initial profile of the vibration displacement is obtained by the force balance equation at the static state, which is written as $u(x, 0) = -(\rho xg + Mg)/E_A$. The initial velocity is defined as $u_t(x, 0) = 0$ because the initial velocity of the each point in the cable is zero. The initial conditions $u(x, 0)$ and $u_t(x, 0)$ used in the simulation satisfy the conditions in Theorem 1. The closed-loop responses with the proposed control law (118) and the proportional–derivative (PD) control law, which is classically utilized in industries, are examined to compare their performance to suppress the axial vibrations of the mining cable. The PD control law is

$$U_{pd}(t) = k_pu(l(t),t) + k_d\dot{u}(l(t),t) \quad (157)$$

where k_p and k_d are gain parameters. The values of k_p and k_d are tuned to attain the efficient control performance. We have tested

Table 1 Physical parameters of the mining cable elevator

Parameters (units)	values
Initial length L (m)	2000
Final length (m)	200
Cable effective steel area A_a (m^2)	0.47×10^{-3}
Cable effective Young's modulus E (N/m^2)	1.03×10^{10}
Cable linear density ρ (kg/m)	8. 1
Total hoisted mass M (kg)	15,000
Gravitational acceleration g (m/s^2)	9.8
Maximum hoisting velocities $V_{\max}$ (m/s)	15
Total hoisting time t_f (s)	150

Downloaded From: http://dynamicsystems.asmedigitalcollection.asme.org/ on 06/16/2018 Terms of Use: http://www.asme.org/about-asme/terms-of-use

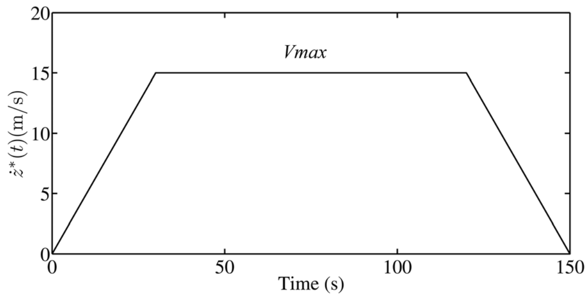

Fig. 2 The hoisting velocity $\dot{z}^*(t)$

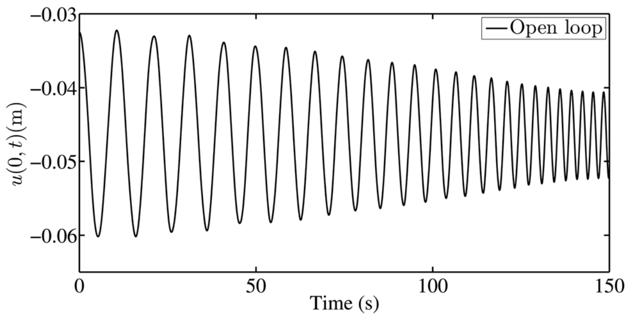

(*a*)

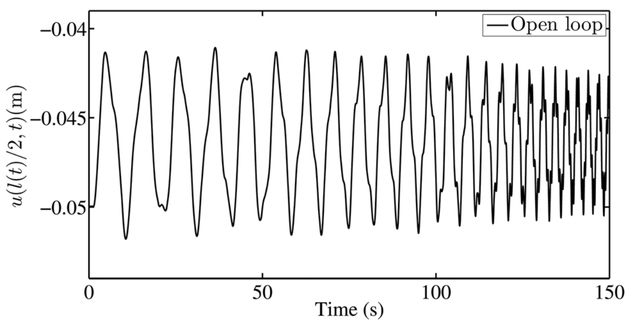

(*b*)

Fig. 3 The open-loop responses of the plant Eqs. (27)–(30). The large vibration is caused both at the moving cage and at the midpoint of the cable: (*a*) the axial vibration at the moving cage and (*b*) the axial vibration at the midpoint.

different values of k_p and k_d, and the best regulating performance is achieved with $k_p = 2000$, $k_d = 7000$ considering the overshoot and adjusting time. The gains of the proposed controller d, $\overline{d}$ and $K = [k_1, k_2]$ are chosen as $d = \overline{d} = 1$ and $[k_1, k_2] = [0.0035, 0.03]$ in the simulation. The numerical simulation is performed by the finite difference method for the discretization in time and space after converting the time-varying domain PDE to the PDE on a fixed domain [0, 1] but with time-varying coefficients by introducing $\hat{\eta} = x/l(t)$ [4]. The time-step and space step are chosen as 0.001 and 0.01, respectively.

6.1 The Vibration Suppression by the Proportional–Derivative Control and the Proposed Control Law. Figure 3 shows the open-loop responses of the plant (27)–(30). It illustrates that the large vibration is caused at both the cage and the midpoint of the string during the total hoisting time. To suppress the vibration, the closed-loop responses with the PD control law (157) and the proposed control law are investigated and shown in Fig. 4. It shows the vibration is suppressed and converges to zero on both the proposed control law and the PD control. Moreover, it can be observed that the responses with the proposed control law have faster convergence and less overshoot than the responses with the

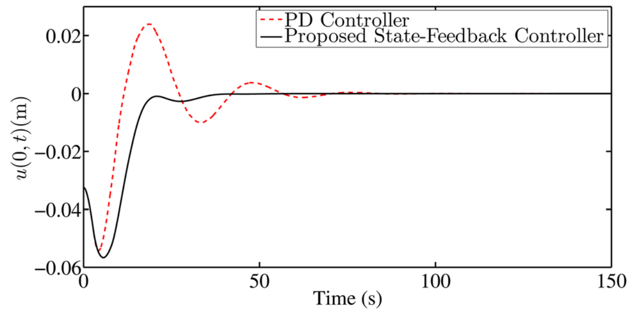

(*a*)

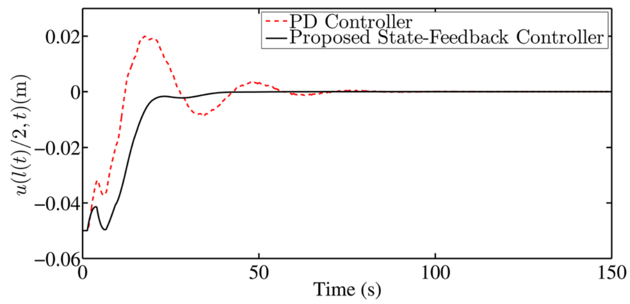

(*b*)

Fig. 4 The closed-loop responses of the plant Eqs. (27)–(30) with the PD controller (157) (dashed line) and the proposed state-feedback controller (61). While both controllers achieve the convergence to zero, the proposed controller achieves faster convergence with less overshoot: (*a*) the axial vibration at the moving cage and (*b*) the axial vibration at the midpoint of the cable.

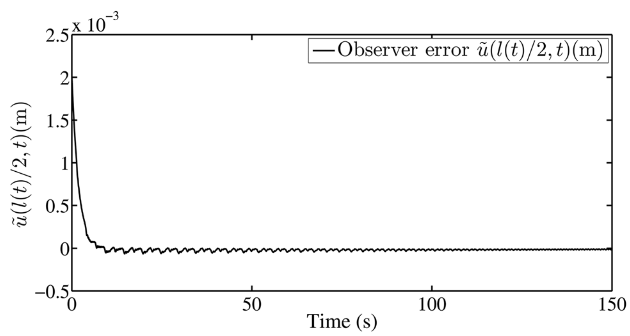

(*a*)

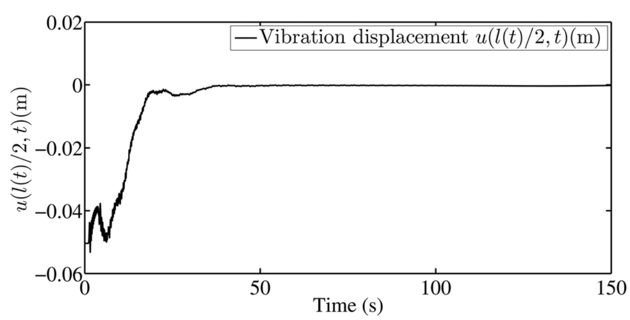

(*b*)

Fig. 5 The responses of the closed-loop system Eqs. (27)–(30) and the observer design Eqs. (75)–(78) with the output-feedback control law (118). The observer achieves convergence to the actual distributed state, and the associated output-feedback controller retains similar performance to the state-feedback: (*a*) the observer error of the axial vibration at the midpoint and (*b*) the axial vibration at the midpoint.

Downloaded From: http://dynamicsystems.asmedigitalcollection.asme.org/ on 06/16/2018 Terms of Use: http://www.asme.org/about-asme/terms-of-use

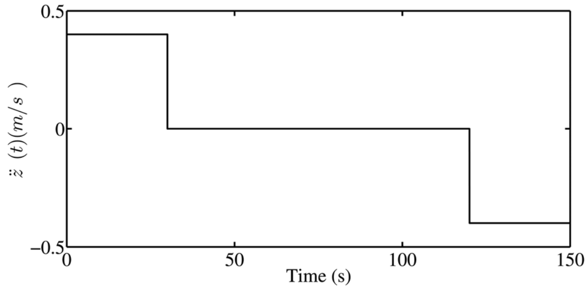

Fig. 6 The hoisting acceleration

PD control law. Thus, the proposed control law shows better performance than the classical PD control.

6.2 The Responses With the Observer-Based Output-Feedback Control Law. With the available boundary measurements of the displacement and the velocity of the axial vibration at the cage $u(0, t)$ and $u_t(0, t)$, the estimated variables of the distributed states required in the control law are obtained by the proposed observer (75)–(78). The closed-loop responses with an observer-based output-feedback controller are simulated with the initial observer error $\tilde{u}(x, 0) = 0.002(\mathrm{m})$ uniformly. Then the initial conditions of the observer used in the simulation are $\hat{u}(x, 0) = u(x, 0) + 0.002$ and $\hat{X}(0) = X(0) + [0.002, 0]^{\mathrm{T}}$, which satisfy the conditions in Theorem 1. The dynamics of the observer error and the vibration displacement at the midpoint of the string are shown in Figs. 5(*a*) and 5(*b*), respectively. Because the locations of the actuator and the sensor are at the opposite boundaries, the stabilization and the estimation of the vibration at the midpoint $x = l(t)/2$ is most challenging due to its accessibility. Figure 5(*a*) shows the observer error converges to zero quickly, which implies that the estimation of the vibration displacements reconstructs their actual distributed states. Figure 5(*b*) shows that the convergence to zero of the vibration state at the midpoint is achieved with the output-feedback control law as well, although the initial observer error affects the controller performance in the initial stage compared with the state-feedback response in Fig. 4.

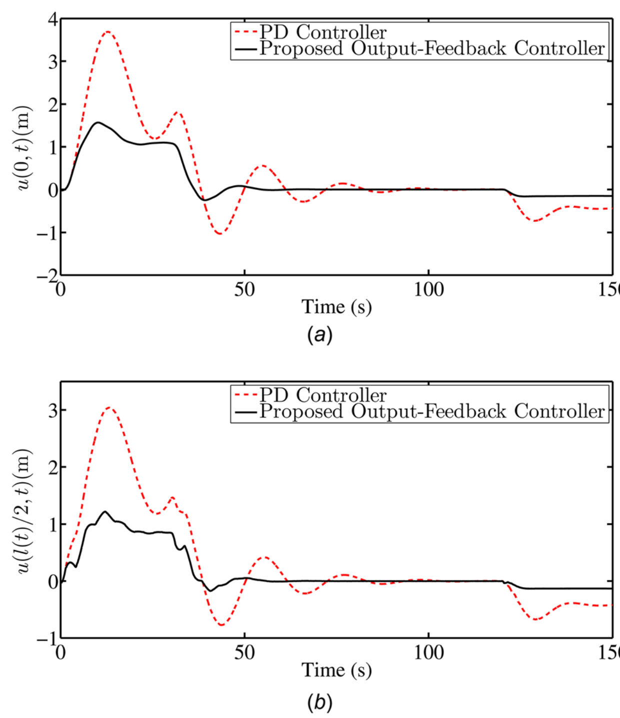

Fig. 7 The closed-loop responses of the accurate plant Eqs. (11)–(13) with Eq. (18) under the PD controller (157) (dashed line) and the proposed output-feedback controller (118): (*a*) the axial vibration at the moving cage and (*b*) the axial vibration at the midpoint of the cable

6.3 The Responses of the Accurate Model. We process the controller design and stability analysis based on the simplified model. In this section, we test the performance of our controller based on the accurate model (11)–(13) with Eq. (18), which includes the boundary and distributed force disturbances from the motion acceleration $\ddot{z}^*(t)$ shown in Fig. 6. Applying the proposed output-feedback controller used in Sec. 6.2 and the PD controller with the coefficients $k_p = 3500$, $k_d = 9000$ which are adjusted to obtain efficient performance, the results under the two controllers are compared in Fig. 7. We can see that our controller also has the better performance on vibration suppression than the PD controller even though considering the boundary and distributed force disturbances from the motion acceleration $\ddot{z}^*(t)$, which would introduce saltation at 30 s and 120 s.

7 Conclusion and Future Work

In this paper, we propose an observer-based output-feedback control design for the axial vibration suppression of a varying-length mining cable with a cage. The dynamics is represented as a coupled wave PDE-ODE system with a Neumann type interconnection on a time-varying spatial domain. The proposed control design is practical for the installation of the actuator and sensor in the mining cable elevator, in which the actuator is located not at the moving cage but at the fixed boundary where a hydraulic actuator acts on a floating sheave. Exponential stability of the closed-loop system with the proposed observer-based output-feedback control law has been proved by Lyapunov analysis. The simulation results verify the theoretical analysis and illustrate that the proposed control law can effectively suppress the axial vibrations of the mining cable elevator. In future work, uncertainties and unknown parameters in the dynamic model of the mining cable elevator will be dealt with in the control design.

Funding Data

- National Basic Research Program of China (973 Program) (Grant No. 2014CB049404).
- Fundamental Research Funds for the Central Universities (Grant No. 106112016CDJXY330002).
- China Scholarship Council (CSC) and Chongqing University Postgraduates' Innovation Project (CYD15023).

Nomenclature

A_a = cross-sectional area of the cable
c_1 = cage-guide damping coefficient
c_2 = cable-head sheave damping coefficient
E = Young's modulus of the cable
g = gravitational acceleration
J_D = moment of inertia of the drum
$l(t)$ = time-varying length of the cable
L = initial length of the cable
M = mass of the load
R_D = radius of the drum
$u(x, t)$ = axial vibration displacement
ρ = linear density of the cable

Appendix

The inverse transformation is defined as

$$u(x,t) = w(x,t) - \int_0^x \varphi(x,y)w(y,t)dy - \int_0^x \lambda(x,y)w_t(y,t)dy - \alpha(x)X(t) \tag{A1}$$

Downloaded From: http://dynamicsystems.asmedigitalcollection.asme.org/ on 06/16/2018 Terms of Use: http://www.asme.org/about-asme/terms-of-use

where kernel functions $\varphi(x, y) \in R$, $\lambda(x, y) \in R$ and $\alpha(x) \in \mathbb{R}^{1\times 2}$ are to be determined. Taking second derivatives of Eq. (A1) with respect to x and t respectively, and substituting them into Eq. (33), we get

$$\begin{aligned} u_{tt}(x,t) - qu_{xx}(x,t) &= 2q(\varphi_y(x,x) + \varphi_x(x,x))w(x,t) \\ &+ q\int_0^x (\lambda_{xx}(x,y) - \lambda_{yy}(x,y))w_t(y,t)dy \\ &+ q\int_0^x (\varphi_{xx}(x,y) - \varphi_{yy}(x,y))w(y,t)dy \\ &+ 2q(\lambda_x(x,x) + \lambda_y(x,x))w_t(x,t) \\ &- (\alpha(x)\tilde{A}B - q\varphi(x,0))w_x(0,t) \\ &+ (q\lambda(x,0) - \alpha(x)B)w_{xt}(0,t) \\ &+ (q\alpha''(x) - \alpha(x)\tilde{A}^2)X(t) = 0 \end{aligned} \tag{A2}$$

where $\tilde{A} = A + BK$. Recall the ODE (32) in the system (32)–(35)

$$\begin{aligned} \dot{X}(t) &= AX(t) + Bu_x(0,t) \\ &= AX(t) + Bw_x(0,t) - B\alpha'(0)X(t) \\ &= (A + BK)X(t) + Bw_x(0,t) \end{aligned} \tag{A3}$$

Considering the boundary condition (34), we get

$$u(0,t) = w(0,t) - \alpha(0)X(t) = \mathrm{C}X(t) \tag{A4}$$

According to Eqs. (A2)–(A4), we get the following conditions on the kernel functions in the inverse transformation:

$$\varphi_y(x,x) + \varphi_x(x,x) = 0 \tag{A5}$$

$$\lambda_y(x,x) + \lambda_x(x,x) = 0 \tag{A6}$$

$$\varphi_{yy}(x,y) - \varphi_{xx}(x,y) = 0 \tag{A7}$$

$$\lambda_{yy}(x,y) - \lambda_{xx}(x,y) = 0 \tag{A8}$$

$$\alpha''(x) - q\alpha(x)\tilde{A}^2 = 0 \tag{A9}$$

$$q\lambda(x,0) - \alpha(x)B = 0 \tag{A10}$$

$$q\varphi(x,0) - \alpha(x)\tilde{A}B = 0 \tag{A11}$$

$$-\alpha'(0) = K \tag{A12}$$

$$-\alpha(0) = C \tag{A13}$$

According to Eqs. (A9), (A12), and (A13), the solution of $\alpha(x)$ can be obtained as

$$\alpha(x) = \begin{bmatrix} -C & -K \end{bmatrix} e^{Zx} \begin{bmatrix} I \\ 0 \end{bmatrix} \tag{A14}$$

where

$$Z = \begin{bmatrix} 0 & q\tilde{A}^2 \\ I & 0 \end{bmatrix}$$

Considering Eqs. (A10), (A11), and (A14), we can get

$$\varphi(x,y) = \frac{1}{q}\begin{bmatrix} -C, & -K \end{bmatrix} e^{Z(x-y)} \begin{bmatrix} I \\ 0 \end{bmatrix} \tilde{A}B \tag{A15}$$

$$\lambda(x,y) = \frac{1}{q}\begin{bmatrix} -C, & -K \end{bmatrix} e^{Z(x-y)} \begin{bmatrix} I \\ 0 \end{bmatrix} B \tag{A16}$$

References

[1] Zhu, W., and Zheng, N., 2008, "Exact Response of a Translating String With Arbitrarily Varying Length Under General Excitation," ASME J. Appl. Mech., **75**(3), p. 031003.
[2] Kaczmarczyk, S., and Ostachowicz, W., 2003, "Transient Vibration Phenomena in Deep Mine Hoisting Cables—Part 1: Mathematical Model," J. Sound Vib., **262**(2), pp. 219–244.
[3] Zhu, W., and Ni, J., 2000, "Energetics and Stability of Translating Media With an Arbitrarily Varying Length," ASME J. Vib. Acoust., **122**(3), pp. 295–304.
[4] Wang, J., Pi, Y., Hu, Y., and Gong, X., 2017, "Modeling and Dynamic Behavior Analysis of a Coupled Multi-Cable Double Drum Winding Hoister With Flexible Guides," Mech. Mach. Theory, **108**, pp. 191–208.
[5] Kaczmarczyk, S., and Ostachowicz, W., 2003, "Transient Vibration Phenomena in Deep Mine Hoisting Cables—Part 2: Numerical Simulation of the Dynamic Response," J. Sound Vib., **262**(2), pp. 245–289.
[6] Nguyen, Q. C., and Hong, K.-S., 2010, "Asymptotic Stabilization of a Nonlinear Axially Moving String by Adaptive Boundary Control," J. Sound Vib., **329**(22), pp. 4588–4603.
[7] Nguyen, Q. C., and Hong, K.-S., 2012, "Simultaneous Control of Longitudinal and Transverse Vibrations of an Axially Moving String With Velocity Tracking," J. Sound Vib., **331**(13), pp. 3006–3019.
[8] Nguyen, Q. C., and Hong, K.-S., 2012, "Transverse Vibration Control of Axially Moving Membranes by Regulation of Axial Velocity," IEEE Trans. Control Syst. Technol., **20**(4), pp. 1124–1131.
[9] He, W., and Ge, S. S., 2015, "Vibration Control of a Flexible String With Both Boundary Input and Output Constraints," IEEE Trans. Control Syst. Technol., **23**(4), pp. 1245–1254.
[10] He, W., Zhang, S., and Ge, S. S., 2014, "Adaptive Control of a Flexible Crane System With the Boundary Output Constraint," IEEE Trans. Ind. Electron., **61**(8), pp. 4126–4133.
[11] Zhang, S., He, W., and Ge, S. S., 2012, "Modeling and Control of a Nonuniform Vibrating String Under Spatiotemporally Varying Tension and Disturbance," IEEE/ASME Trans. Mechatronics, **17**(6), pp. 1196–1203.
[12] Ge, S. S., He, W., How, B. V. E., and Choo, Y. S., 2010, "Boundary Control of a Coupled Nonlinear Flexible Marine Riser," IEEE Trans. Control Syst. Technol., **18**(5), pp. 1080–1091.
[13] He, W., and Ge, S. S., 2016, "Cooperative Control of a Nonuniform Gantry Crane With Constrained Tension," Automatica., **66**, pp. 146–154.
[14] Curtain, R., and Morris, K., 2009, "Transfer Functions of Distributed Parameter Systems: A Tutorial," Automatica, **45**(5), pp. 1101–1116.
[15] Sandilo, S. H., and van Horssen, W. T., 2014, "On Variable Length Induced Vibrations of a Vertical String," J. Sound Vib., **333**(11), pp. 2432–2449.
[16] Zhu, W., Ni, J., and Huang, J., 2001, "Active Control of Translating Media With Arbitrarily Varying Length," ASME J. Vib. Acoust., **123**(3), pp. 347–358.
[17] He, W., Nie, S., Meng, T., and Liu, Y.-J., 2017, "Modeling and Vibration Control for a Moving Beam With Application in a Drilling Riser," IEEE Trans. Control Syst. Technol., **25**(3), pp. 1036–1043.
[18] He, W., Ge, S. S., and Huang, D., 2015, "Modeling and Vibration Control for a Nonlinear Moving String With Output Constraint," IEEE/ASME Trans. Mechatronics, **20**(4), pp. 1886–1897.
[19] Krstic, M., Guo, B.-Z., Balogh, A., and Smyshlyaev, A., 2008, "Output-Feedback Stabilization of an Unstable Wave Equation," Automatica, **44**(1), pp. 63–74.
[20] Krstic, M., and Smyshlyaev, A., 2008, *Boundary Control of PDEs: A Course on Backstepping Designs*, SIAM, Singapore.
[21] Bekiaris-Liberis, N., and Krstic, M., 2014, "Compensation of Wave Actuator Dynamics for Nonlinear Systems," IEEE Trans. Autom. Control, **59**(6), pp. 1555–1570.
[22] Krstic, M., 2010, "Adaptive Control of an Anti-Stable Wave PDE," Dynam. Cont. Dis. Ser. A, **17**, pp. 853–882.
[23] Bresch-Pietri, D., and Krstic, M., 2014, "Output-Feedback Adaptive Control of a Wave PDE with Boundary Anti-Damping," Automatica, **50**(5), pp. 1407–1415.
[24] Krstic, M., 2009, "Compensating Actuator and Sensor Dynamics Governed by Diffusion PDEs," Syst. Control Lett., **58**(5), pp. 372–377.
[25] Krstic, M., 2009, "Compensating a String PDE in the Actuation or Sensing Path of an Unstable ODE," IEEE Trans. Autom. Control, **54**(6), pp. 1362–1368.
[26] Hasan, A., Aamo, O., and Krstic, M., 2016, "Boundary Observer Design for Hyperbolic PDE-ODE Cascade Systems," Automatica, **68**, pp. 75–86.
[27] Aamo, O., 2013, "Disturbance Rejection in 2 × 2 Linear Hyperbolic Systems," IEEE Trans. Autom. Control, **58**(5), pp. 1095–1106.
[28] Ren, B., Wang, J.-M., and Krstic, M., 2013, "Stabilization of an ODE–Schrödinger Cascade," Syst. Control Lett., **62**(6), pp. 503–510.
[29] Tang, S., and Xie, C., 2011, "Stabilization for a Coupled PDE-ODE Control System," J. Franklin Inst., **348**(8), pp. 2142–2155.
[30] Cai, X., and Krstic, M., 2015, "Nonlinear Control Under Wave Actuator Dynamics With Time-and State-Dependent Moving Boundary," Int. J. Rob. Nonlinear, **25**(2), pp. 222–251.
[31] Cai, X., and Krstic, M., 2016, "Nonlinear Stabilization Through Wave PDE Dynamics With a Moving Uncontrolled Boundary," Automatica, **68**, pp. 27–38.
[32] Susto, G. A., and Krstic, M., 2010, "Control of PDE–ODE Cascades With Neumann Interconnections," J. Franklin Inst., **347**(1), pp. 284–314.

Downloaded From: http://dynamicsystems.asmedigitalcollection.asme.org/ on 06/16/2018 Terms of Use: http://www.asme.org/about-asme/terms-of-use

[33] Tang, S., and Xie, C., 2011, "State and Output Feedback Boundary Control for a Coupled PDE–ODE System," Syst. Control Lett., **60**(8), pp. 540–545.
[34] Zhou, Z., and Tang, S., 2012, "Boundary Stabilization of a Coupled Wave-ODE System With Internal Anti-Damping," Int. J. Control, **85**(11), pp. 1683–1693.
[35] McIver, D. B., 1973, "Hamilton's Principle for Systems of Changing Mass," J. Eng. Math., **7**(3), pp. 249–261.
[36] Bresch-Pietri, D., and Krstic, M., 2014, "Adaptive Output Feedback for Oil Drilling Stick-Slip Instability Modeled by Wave PDE With Anti-damped Dynamic Boundary," American Control Conference (ACC), Portland, OR, June 4–6, pp. 386–391.
[37] Krstic, M., 2009, *Delay Compensation for Nonlinear, Adaptive, and PDE Systems*, Birkhäuser, Boston, MA.
[38] Roman, C., Bresch-Pietri, D., Cerpa, E., Prieur, C., and Sename, O., 2016, "Backstepping Observer Based-Control for an Anti-Damped Boundary Wave PDE in Presence of In-Domain Viscous Damping," 55th Conference on Decision and Control (CDC), Las Vegas, NV, Dec. 12–14, pp. 549–554.
[39] Wang, J., Krstic, M., and Pi, Y., "Control of a 2×2 Coupled Linear Hyperbolic System Sandwiched Between Two ODEs," Int. J. Robust Nonlinear (to appear).
[40] Krstic, M., 2011, "Dead-Time Compensation for Wave/String PDEs," ASME J. Dyn. Syst. Meas. Control, **133**(3), p. 031004.

Downloaded From: http://dynamicsystems.asmedigitalcollection.asme.org/ on 06/16/2018 Terms of Use: http://www.asme.org/about-asme/terms-of-use